



Contents lists available at ScienceDirect

Acta Ecologica Sinica

journal homepage: www.elsevier.com/locate/chnaes

Analysis of land cover land use change in the greater Gaborone area of South Eastern Botswana

Celestine Neba Suh^{a,*}, Rejoice Tsheko^a, Benedict Kayombo^a, Scott Thebeetsile Moroke^b^a Department of Agricultural and Biosystems Engineering, Botswana University of Agriculture and Natural Resources, Gaborone, Botswana.^b Department of Crop and Soil Sciences, Botswana University of Agriculture and Natural Resources, Gaborone, Botswana

ARTICLE INFO

Keywords:

Land cover land use
Image classification
Change detection
Annual change rate
Conversion

ABSTRACT

Changes in land cover land use (LCLU) have long been considered to be among the many factors responsible for global environmental challenges. This study focused on assessing LCLU changes in the Greater Gaborone area of South Eastern Botswana between 1988 and 2022. The study employed remote sensing (RS) and geographic information systems (GIS) tools for analyzing LCLU changes in the study area during the study period. Landsat images of 1988 and 2002 and Sentinel-2A images of 2022 were used to detect LCLU changes. Image classification was done using a Supervised classification approach based on a Maximum Likelihood Classifier. Six LCLU types such as water body, trees dominated, cropland, shrubland, bare land, and built-up, were identified in the area. Post Classification Comparison (PCC) approach was used to detect LCLU change during the study period. Shrubland class was found to be the dominant LCLU type in the study area. A significant gain was observed in the built-up class (75.12 km²), while significant losses were observed in shrubland (24.16 km²) and trees dominated (33.32 km²) classes in the entire study period. Given the rapid increase in built-up areas, this recommends that land managers and policymakers should invest in implementing sustainable land management interventions to prevent undesirable LCLU changes.

1. Introduction

Land cover land use change (LCLU) is one of the driving forces of environmental change increasingly becoming a global concern due to its impact on the local, regional and global environment [1,2]. LCLU change refers to the modification of the earth's terrestrial surface due to complex interactions between humans and the physical environment [3]. These changes are historically linked to the variation in biophysical factors, while recent changes are associated with anthropogenic activities [4,5]. Over the past decades, humans had increasingly taken a large role in modifying the environment [6]. With the increasing number of developing technologies, man has emerged as a major and most powerful instrument of environmental change [7].

Drivers of LCLU change vary over time and so are their impacts [8]. These drivers are broadly classified into two categories: proximate and underlying drivers. Proximate (or direct) causes are linked to the immediate actions taken by humans to meet their needs through land use. These include agricultural expansion, wood extraction, infrastructural expansion etc., altering the physical state [9]. The underlying (or

indirect) drivers, on the other hand, are related to fundamental socio-economic and political processes that push proximate causes into immediate action [9]. At the proximate level, changes in LCLU could be explained by multiple factors rather than a single variable [9]. Proximate causes operate at the local level (individual farms, householders, or communities), whereas underlying causes are prevalent at regional and national levels such as districts, provinces, or countries [8]. Understanding the proximate and underlying drivers is essential for analyzing LCLU change, as well as developing realistic models for simulating future LCLUs and changes [10].

Monitoring LCLU changes is vital because failure to do so, could result in severe environmental challenges such as climate change, biodiversity loss (due to habitat fragmentation), and pollution among others. Seasonal changes caused by climate change could contribute to poverty intensification, severely affecting the economy of a country, as more funds are likely to be channelled towards poverty alleviation at the expense of other developmental projects [11]. Therefore, monitoring LCLU changes is essential for the sustainable management of natural resources by formulating policies that strike a balance between

* Corresponding author.

E-mail addresses: Suhcelestine28@gmail.com (C.N. Suh), rtsheko@buan.ac.bw (R. Tsheko), bkayombo@buan.ac.bw (B. Kayombo), tmoroke@buan.ac.bw (S.T. Moroke).

<https://doi.org/10.1016/j.chnaes.2023.03.004>

Received 27 October 2022; Received in revised form 20 March 2023; Accepted 22 March 2023

1872-2032/© 2023 Ecological Society of China. Published by Elsevier B.V. All rights reserved.

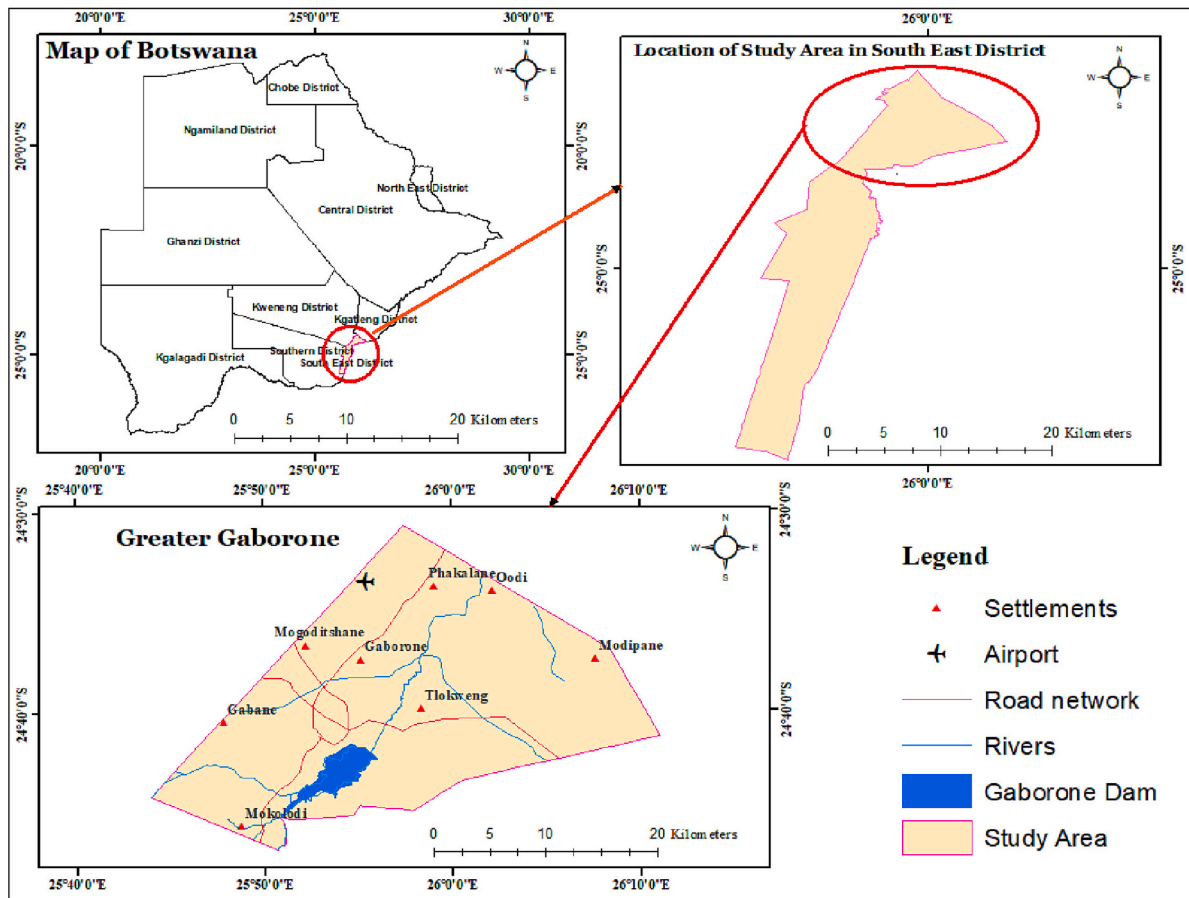


Fig. 1. Map of the study area [17].

conservation, conflicting uses, and development-oriented pressures.

Studies from Sub-Saharan Africa (SSA) and other developing countries have shown that agriculture expansion, population growth, poverty and unsustainable use of natural resources are responsible for LCLU changes, especially in communities surrounding a natural resource base [12]. In Botswana, LCLU changes are primarily driven by human and livestock population pressures, rapid urbanization and general development activities such as increased demand for arable and grazing land, tourism, water and fuelwood [13].

The Greater Gaborone region in Southeastern Botswana had experienced significant population growth over the past four decades, primarily driven by rural-to-urban migration. Its population grew from 72,127 in 1981 to 429,293 in 2022 [14,15]. According to Keiner and Cavric [16], Gaborone and its surrounding settlements receive the majority of the country's rural-urban migration due to more available job opportunities, better infrastructure, social amenities, and public service. The growing population coupled with the unprecedented economic and industrial development in and around the city of Gaborone over the past decades have contributed to LCLU changes. However, very little is known about the magnitude and rate of LCLU change in the area over the last three decades. This study, therefore, assessed change in LCLUs in the Greater Gaborone area of South Eastern Gaborone between 1988 and 2022 using remote sensing and geographic information system (GIS) applications. The output of this study provides useful information for land use planners to make better decisions within the framework of sustainable land use planning.

Table 1

Population for Gaborone and surrounding villages [14,21].

Location	1981	1991	2001	2011	2022
Gaborone	59,657	133,468	186,007	231,592	246,325
Tlokweng	6657	12,501	21,133	36,323	55,508
Oodi	-	2282	3440	5687	10,257
Modipane	-	-	2508	3197	7945
Mokolodi	-	-	507	624	1242
Mogoditshane	3125	14,246	38,816	57,637	88,006
Gabane	2688	5975	10,399	15,237	20,010
Total population	72,127	168,472	262,810	350,297	429,293

2. Materials and methods

2.1. Description of the study area

The Greater Gaborone area lies between Longitude $25^{\circ} 45' 17.76''$ E and $26^{\circ} 11' 01.04''$ E and Latitude $24^{\circ} 41' 15.44''$ S and $24^{\circ} 42' 45.96''$ S. It covers a surface area of 669 km², with an average elevation of approximately 1000 m above mean sea level (a.m.s.l.). To the east, the area includes the tribal villages of Tlokweng, Oodi and Modipane; to the west, it includes Mogoditshane and Gabane; to the south, it includes Mokolodi; and to the north, Gaborone is bordered by the Kgatleng district (Fig. 1) [17].

These peri-urban villages have grown with the influence of the city and have attained the status of its suburbs, even though their land tenure remains tribal [14]. Historically, a large area of Gaborone City used to be a freehold farmland. For example, the area west of the railway line (now known as Gaborone – West) and Broadhurst did not exist until the early 1980s when the government bought freehold farms in those areas to

Table 2
Images used for LCLU classification and analysis.

Year	Satellite/Sensor	Path/Row	Acquisition date	Resolution (m)	Bands used	Source
1988	Landsat 5 (TM)	172/077	March 19	30*30	1,2,3,4,5,6,7	USGS
2002	Landsat 7 (ETM+)	172/077	March 6	30*30	1,2,3,4,5,6,7	USGS
2022	Sentinel-2 (MSI)	T35JMN	March 30	10*10	2,3,4,8	USGS
2022	Sentinel-2 (MSI)	T35JLN	March 30	10*10	2,3,4,8	USGS

make way for development [14]. Some farms have been developed into huge townships like Pakalane Estates, Gaborone North and Mokolodi. These areas are now fully developed suburbs, well established with all the social amenities that go along with modern residential development. The population of the villages had grown rapidly between 1988 and 2022 (Table 1). The development of these peri-urban villages means that the land is constantly being converted from its natural state to urban status.

The climate of the area is semi-arid, characterized by a hot wet season (November–April), a long dry season (May–October) of which (May–August) is the winter season. The annual average temperature of the area is 20.6 °C, with average minimum and maximum monthly temperatures of 12.8 and 28.6 °C, respectively [18]. The annual average rainfall brought by winds from the Indian Ocean, averages 500 mm [19]. Prolonged dry spells during rainy seasons are common and rainfall is erratic, highly variable and spatially localized [20]. Agricultural practices in the study area include crop and livestock production. Also, permanent water features in the area, include the Gaborone Dam and the wastewater treatment ponds. More so, the vegetation cover mainly consists of *Acacia* shrubs and tree savanna. The most common tree species in the area are *Acacia tortilis* and *Acacia erubescence* [14].

2.2. Methodology

2.2.1. Data acquisition

To detect changes in LCLU classes, this study examined satellite images from Landsat 5 (1988), Landsat 7 (2002), and Sentinel-2A (2022). The images were obtained from the official website of the United States Geological Survey (USGS) Earth Explorer (www.usgs.gov) by accessing path 172 and row 77 for Landsat images and T35JLN/MN for Sentinel-2A (Table 2). The selected images had a cloud cover of less than 10% (for easy interpretation) and were acquired in March for temporal consistency that minimizes seasonal and sun varying position effects. The area of interest (AOI) was digitized in Google Earth Pro, exported as a KML file and converted to a shapefile in ArcGIS 10.7.

2.2.2. Image pre-processing

Landsat images used for LCLU classification are often affected by atmospheric and topographic/geometric errors which have to be corrected [22]. All images were radiometrically and geometrically corrected. Radiometric correction was done by converting digital numbers to radiance using the metadata parameters. Geometric correction, on the other hand, was made possible by ortho-rectifying the images after projecting them to a common geographic reference system. This was defined by the Universal Transverse Mercator (UTM), specifically, UTM zone 35S coordinate on WGS 1984. The study area is covered by one Landsat and two Sentinel-2A image tiles. The two Sentinel images were mosaicked in ArcGIS 10.7 to create a new raster image before the AOI was extracted for classification.

2.2.3. Image classification

In this study, a supervised classification method based on a Maximum Likelihood classifier was used to extract the LCLU classes. This method was chosen because it classifies pixels based on the highest probability that a pixel belongs to a given class. In addition, this method assumes that the spectral values of the training pixels are normally distributed and compute the probability that the given pixel belongs to a

Table 3

Description of LCLU classes in the study area [4,17].

LCLU type	Description
1 Waterbody	Streams, rivers, dams or reservoirs, ponds.
2 Trees dominated	Woody plant more than 5 m in height with a somehow definite crown
3 Cropland	Cropland, forage, orchards, nurseries, horticultural land, fallow land, intensively, moderately and sparsely cultivated lands.
4 Shrub land	Woody plants, less than 5 m in height, no defined crown, a mixture of trees with grasses.
5 Bare land	Exposed soils, sand, bare rocks, with less than 10% vegetation cover, floodplain, quarries, and sparse vegetation.
6 Built-up	Residential, commercial, industrial, transportation and urban areas.

specific class [23].

In the classification process, training classes were selected through visual interpretation of high-resolution satellite images in Google Earth Pro maps. The training areas of each LCLU class were selected using randomised sampling throughout the study area to obtain good representatives [23]. The centers of large patches of LCLU classes that were not likely to contain mixed pixels, were selected to improve the classification accuracy. Using a rule-of-thumb approach, at least 500 pixels per class were selected to enable a meaningful calculation of statistics [24]. Based on the characteristics of the images, six LCLU types were identified. The identified LCLU classes include water bodies, trees dominated, cropland, shrubland, bare land and built-up (Table 3).

2.2.4. Post classification refinement

A classified image often contains noise caused by isolated pixels of some classes, within another dominant class, which can form large patches [25]. It is important to presume that these isolated pixels, more likely belong to this dominating class, than to the classes to which they were initially assigned as a result of classification errors. In this study, tools such as the Majority filter and Boundary clean tools integrated within the ArcGIS software, were used to smoothen or refine the classified images. Post-classification smoothing with a majority filter, reduces unnecessary errors and may further improve classification accuracy [25].

2.2.5. Accuracy assessment

Accuracy assessment in image classification, is essential as it measures the number of ground truth pixels that have been classified correctly – producer accuracy and the expected accuracy when using the created map – user accuracy [11]. In this study, classification accuracy assessment was performed based on points that were identified on the images and selected to represent the different LCLU classes in the study area. A stratified random sampling method was used to collect a total of 232, 274, and 296 reference data from the classified LCLU maps of 1988, 2002, and 2022, respectively. This was done to ensure that all six (6) LCLU classes were adequately represented based on the proportional area of each class. The datasets were imported into Google Earth Pro maps to assess the classification accuracy. The ground truth and the classification data were compared and statistically analyzed through an Error matrix, to determine if the pixels were grouped to the correct

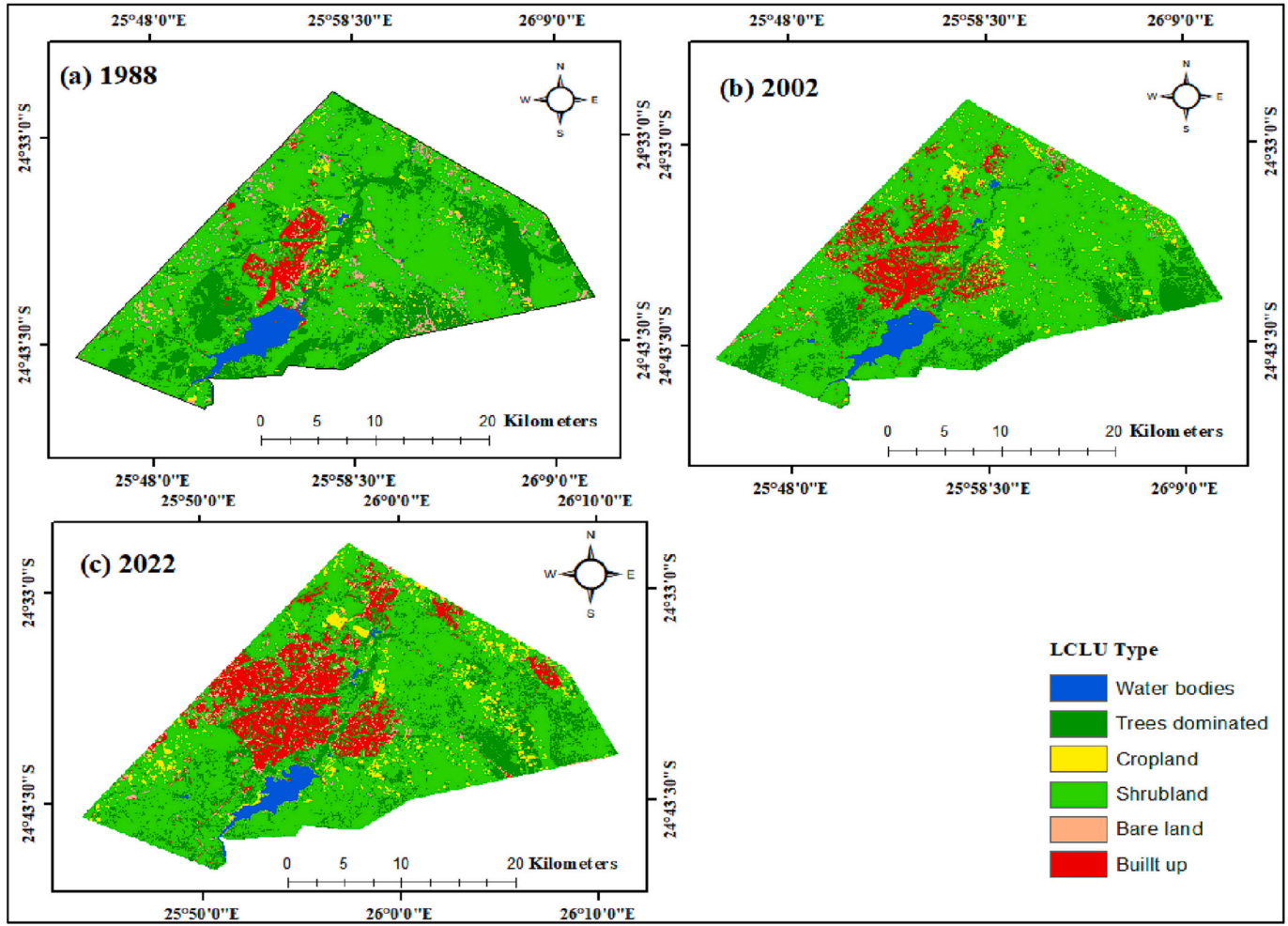


Fig. 2. LCLU categories for (a) 1988, (b) 2002 and (c) 2022.

feature class. The Error matrix was further used to compute the overall accuracy (OA), user's accuracy (UA), producer's accuracy (PA) and Kappa coefficient (KC). The UA, PA and OA were computed using the following equations (1)–(3):

$$UA = \frac{C_{aU}}{C_{a+U}} \times 100 \quad (1)$$

$$PA = \frac{C_{aR}}{C_{a+R}} \times 100 \quad (2)$$

$$OA = \sum_{a=1}^u \frac{C_{aa}}{Q} \times 100 \quad (3)$$

where C_{aU} is the total number of correct classifications of a particular map class; C_{a+U} is the total number of pixels classified in a particular map class; C_{aR} is the number of reference points classified accurately, while C_{a+R} is the total number of reference points in a particular map class and Q is the total number of reference points in the error matrix.

The OA, UA and PA, respectively indicate the accuracy of the entire classification, the likelihood that a pixel classified represents the class on the ground or in reference data, and how well the trained pixels of the given cover type are classified [4]. The KC represents the measure of reproducibility and assesses the probability of chance agreement between the reference and the image datasets [26]. The following eq. (4) derived by Jensen and Cowen [27] was used to compute KC. In Kappa analysis, a KC of 0.8 and above indicates a very strong agreement, while a KC between 0.4 and 0.8 indicates a good agreement, and below 0.4

indicates a poor agreement [28].

$$KC = \frac{N \sum_{i=1}^r X_{ii} - \sum_{i=1}^r (X_{i+} * X_{+i})}{N^2 - \sum_{i=1}^r (X_{i+} * X_{+i})} \quad (4)$$

Where KC is the Kappa coefficient, N is the total number of observations included in the matrix, r is the number of rows in the error matrix, X_{ii} is the number of observations in row i and column i (on the major diagonal), X_{i+} is the total number of observations in row i (shown as marginal total to the right of the matrix), and X_{+i} is the total number of observations in column i (shown as marginal total at bottom of the matrix).

2.2.6. Change detection

Post Classification Comparison (PCC) method was used to detect LCLU changes that previously occurred in the study area. PCC uses pixel-based comparison to generate change information on a pixel-by-pixel basis and thus interpret the changes, more efficiently taking the advantage of “from-to” information [4]. In addition, this approach provides detailed information on the initial and final LCLU types in a complete matrix of change direction [11]. The use of the PCC technique resulted in a cross-tabulation matrix (or LCLU change transition matrix) which was computed using the overlay functions in ArcGIS. The gains and losses in each LULC type between 1988 and 2022 were categorized into three (3) time periods being: (a) 1988–2002, b) 2002–2022 and c) 1988–2022. The following four aspects recommended by Macleod and Congalton [29], were examined after the change detection was performed: assessing the changes that have occurred, identifying the nature

Table 4
Confusion matrix and classification accuracy of LCLU 1988 image.

LCLU Type	Water	Tree cover	cropland	Shrubs	Bare land	Built up	Total User	UA (%)
Water	32	0	0	0	0	0	32	100.0
Tree cover	0	28	1	4	0	0	33	84.8
Cropland	0	1	39	1	0	0	41	95.1
Shrubland	0	6	1	36	2	0	45	80.0
Bare land	0	0	4	0	29	7	40	72.5
Built up	0	0	2	0	4	35	41	85.4
Total Producer	32	35	47	41	35	42	232	
PA (%)	100.0	80.0	83.0	87.8	82.9	83.3		
OA	85.8%							
Kc	0.83							

Table 5
Confusion matrix and classification accuracy of LCLU 2002 image.

LCLU Type	Water	Trees dominated	cropland	Shrubs	Bare land	Built up	Total User	UA (%)
Water	30	0	0	0	0	0	30	100.0
Trees dominated	0	44	0	3	0	0	47	93.6
Cropland	0	0	34	2	2	4	42	81.0
Shrubland	0	3	4	57	0	0	64	89.1
Bare land	0	0	4	1	34	6	45	75.6
Built up	0	0	5	0	4	37	46	80.4
Total Producer	30	47	47	63	40	47	274	
PA (%)	100.0	93.6	72.3	90.5	85.0	78.7		
OA	86.1%							
Kc	0.83							

Table 6
Confusion matrix of 2022 and classification accuracy of LCLU 2022 image.

LCLU Type	Water	Trees dominated	Cropland	Shrubs	Bare land	Built up	Total User	UA (%)
Water	28	0	0	0	0	0	28	100.0
Trees dominated	0	64	0	0	0	0	64	100.0
Cropland	0	0	34	2	0	1	37	91.9
Shrubland	0	2	5	63	0	0	70	90.0
Bare land	0	0	1	0	28	4	33	84.8
Built up	0	0	1	0	2	61	64	95.3
Producer	28	66	41	65	30	66	296	
PA (%)	100.0	97.0	82.9	96.9	93.3	92.4		
OA	94.0%							
Kc	0.93							

of change, calculating the areal extent of change, and assessing the spatial pattern of the change.

2.3. Annual rate of LCLU changes

For each time period, the pattern of change for each LCLU class was calculated, and the magnitude of change in LCLU types within and between time periods was compared. The rate of change was calculated in square kilometers (km²) per year. Also, the percentage (%) share of each LCLU type was calculated to demonstrate the magnitude of change experienced between the periods using the following equations [4,30]:

$$CA = \frac{A_2 - A_1}{A_1} * 100 \quad (5)$$

$$D = \frac{A_2 - A_1}{A_1(T_2 - T_1)} * 100 \quad (6)$$

Where CA is the percentage change in the area of LCLU class between initial time T_1 and final time T_2 , D is the annual average rate of change (%), A_1 is the area of the LCLU class at time 1 (T_1), and A_2 is the area of the LCLU class at time 2 (T_2).

3. Results and discussion

3.1. LCLU types in 1988, 2002 and 2022

The Landsat and Sentinel 2 images obtained from the USGS were classified using Supervised classification employing the Maximum Likelihood algorithm. LCLU maps were developed to show the LCLU types identified in the study area in 1988, 2002 and 2022. The detected LCLU types were water bodies, trees dominated, cropland, shrubland, bare land and built-up land (Fig. 2). Accuracy assessment for the three LCLU classification images was done by comparing the classification results with ground truth points. Error matrix was used to compute the UA, PA, OA and KC for 1988, 2002 and 2022 LCLU maps and the results are presented in Tables 4, 5 and 6. The overall classification accuracy for the 1988, 2002 and 2022 images, were 85.8%, 86.1% and 94.0%, respectively. These values are acceptable as OA statistics normally fall between 85% and 95%, according to Macleod and Congalton [29]. The KCs obtained for the 1988, 2002 and 2022 images, were 0.83, 0.83 and 0.93, respectively. These Kappa coefficients were greater than 0.8, indicating a high level of agreement between image data and ground truth data, as stated by Molla et al. [28].

Table 7

Area Statistics for the LCLU categories in 1988, 2002 and 2022.

LCLU types	LCLU 1988		LCLU 2002		LCLU 2022	
	Area (km ²)	Area (%)	Area (km ²)	Area (%)	Area (km ²)	Area (%)
Water bodies	22.19	3.32	19.54	2.92	15.43	2.31
Trees dominated	129.68	19.39	107.58	16.08	96.42	14.41
Cropland	39.73	5.94	20.93	3.13	33.47	5
Shrubland	426.47	63.75	438.35	65.53	402.57	60.18
Bare land	26.65	3.98	8.95	1.34	21.63	3.23
Built up	24.22	3.62	73.59	11	99.41	14.86
Total	668.94	100	668.94	100	668.94	100

3.2. Area statistics for LCLU types in 1988, 2002 and 2022

From Table 7 and Fig. 3, the shrubland class was found to be the most dominant LCLU class in the study area, covering an area of 426.47 km² (63.75%) in 1988, 438.35 km² (65.53%) in 2002 and 402.57 km² (60.18%) in 2022. The trees dominated LCLU type occupied an area of 129.68 km² (19.39%) in 1988, 107.58 km² (16.08%) in 2002, and 96.42 km² (14.41%) in 2022. In 1988 and 2002, the trees dominated class was the second most dominant class in the study area after the shrubland class. The built-up class occupied an area of 24.22 km² (3.62%) in 1988, 73.59 km² (11%) in 2002, and 99.41 km² (14.86%) in 2022. The built-up class was the second most dominant LCU type after the shrubland class in the area in 2022.

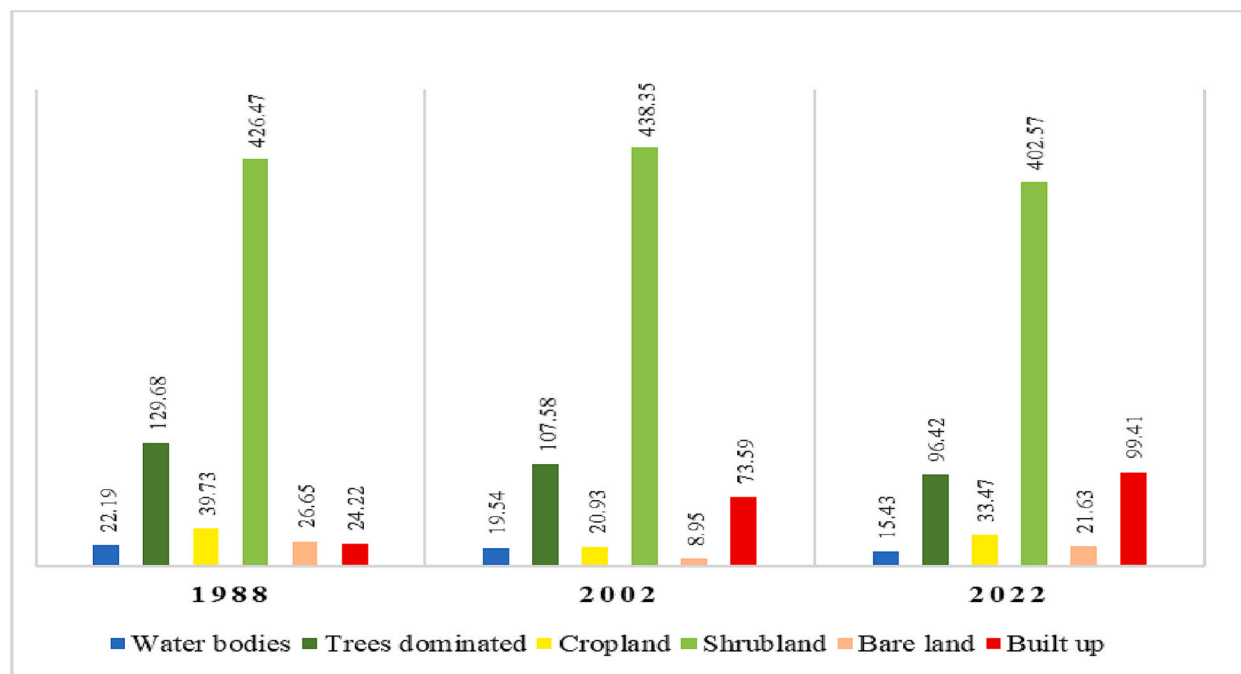
The bare land class accounted for 26.65 km² (3.98%) of the total land area in 1988, 8.95 km² (1.34%) in 2002, and 21.62 km² (3.23%) in 2022. Bare land was the least dominant class in the area in 2002. The cropland class occupied 39.73 km² (5.94%) of the total land area in 1988, 20.93 (3.13%) in 2002, and 33.45 km² (5%) in 2022. The water body class covered an area of 22.19 km² (3.32%) in 1988, 19.54 km² (2.92%) in 2002 and 15.42 km² (2.31%) in 2022. It was the least dominant class in the area in 2022.

3.3. Gains and losses in LCLU types

Conversions from one type of LCLU to another were observed throughout the study period (Fig. 4, Fig. 5). Generally, the spatial extent of an LCLU type decreases once its portion is converted into another type. Gains and losses in the area coverage for the different LCLU types, were assessed using the LCLU change matrix (Tables 8, 9 and 10). From the results, the built-up class gained primarily from the shrubland class throughout the study period. It gained 34.97 km² of shrubland between 1988 and 2002 (Table 8) and 49.21 km² between 2002 and 2022 (Table 9), thereby increasing its spatial extent. Overall, the built-up class gained 75.12 km² throughout the entire study period (Fig. 5). The expansion in built-up areas could be attributed to population growth due to rural-urban migration, resulting in the conversion of areas previously used for agriculture or other purposes, into residential areas.

The bare land class lost 17.41 km² of its area to the shrubland class between 1988 and 2002 (Table 8), which could be attributed to vegetation regrowth due to heavy rains experienced in the country after prolonged drought period of 1993–1995 [31]. However, between 2002 and 2022, the bare land class gained 14.1 km² from the shrubland class (Table 9). This could be attributed to the interaction of both climates (such as drought) and human activities (livestock grazing and land clearing for fuelwood and cultivation), resulting in the loss of vegetal cover [32,33].

The area coverage of the trees dominated class decreased throughout the study period, and this was due to its conversion to the shrubland class. The most common tree species found in the study area were, *Acacia tortilis* and *Acacia erubescence*. Other tree species such as *Combretum imberbe* and *Terminalia prunioides*, were common in the 1980s but had been depleted because they were the most preferred species for fuelwood [14]. Even though the shrubland LCLU type was generally losing its area coverage, a significant gain (11.88 km², 2.79%) in its cover was observed between 1988 and 2002. The gain in shrubland during this period was mainly from the trees dominated class (due to forest clearing for fuelwoods and other forest products) and bare land. The gain in shrubland from bare land, indicated the ability of natural vegetation to regenerate even after extended periods of drought. Between 2002 and 2022, a significant loss in the area coverage of the

**Fig. 3.** Area Statistics for the LCLU types in 1988, 2002 and 2022.

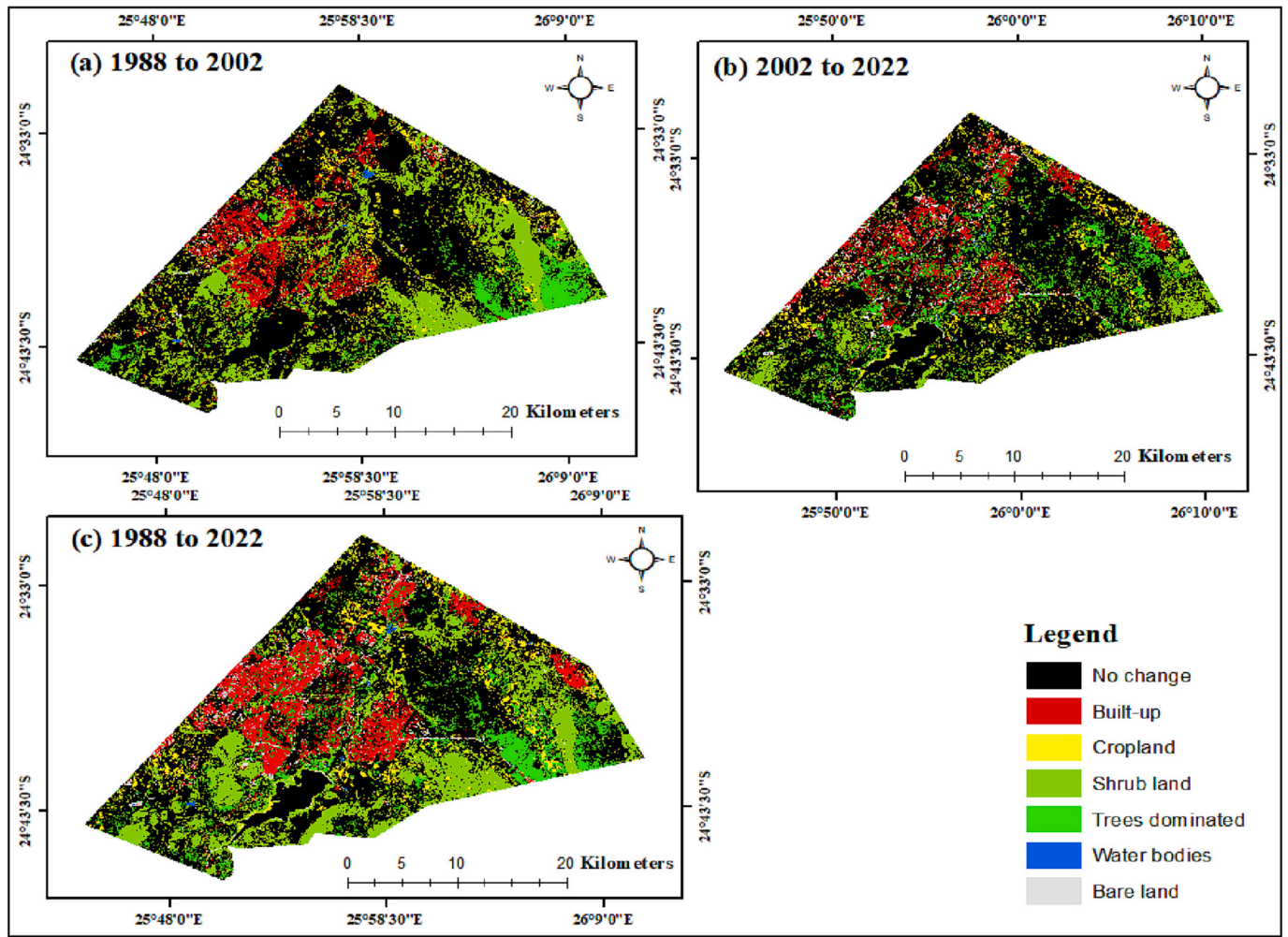


Fig. 4. Changes in LCLU types from (a) 1988 to 2002; (b) 2002 to 2022 and (c) 1988 to 2022.

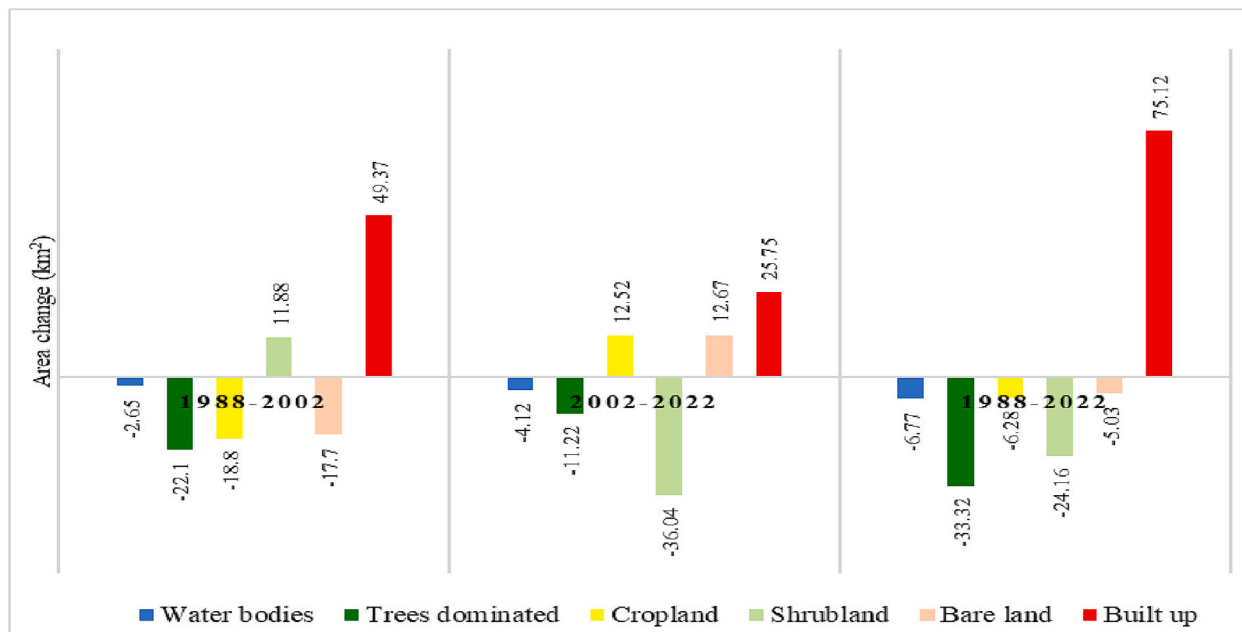


Fig. 5. Gains and losses in LCLU classes from 1988 to 2022.

Table 8

LCLU change matrix for 1988–2002 change period.

1988	LCLU classes	2002							
	Water bodies	Water bodies	Trees dominated	Cropland	Shrub land	Bare land	Built-up	Losses (km ²)	Losses (%)
Water bodies	19.43	0.48	0.06	1.84	0.01	0.38	2.77	12.47	
Trees dominated	0.51	34.44	2.01	107.34	0.65	3.37	113.88	76.78	
Cropland	0.03	0.51	3.24	20.98	0.28	1.61	23.41	87.83	
Shrubland	0.3	36.16	12.11	331.03	6.31	34.97	95.63	22.41	
Bare land	0.07	0.24	3.26	17.41	1.25	4.4	25.4	95.31	
Built-up	0.02	0.03	0.19	4.54	0.27	19.19	5.05	20.85	
Gains (km ²)	0.93	37.43	17.63	146.33	7.52	44.73	266.14		
Gains (%)	4.55	52.08	87.83	30.65	85.76	69.98			

Table 9

LCLU change matrix for 2002–2022 change period.

2002	LCLU classes	2022							
	Water bodies	Water bodies	Trees dominated	Cropland	Shrub land	Bare land	Built-up	Losses (km ²)	Losses (%)
Water bodies	15.07	0.25	0.98	3.18	0.87	0.01	5.28	25.96	
Trees dominated	0.04	30.28	0.61	64.1	0.30	0.54	65.59	68.42	
Cropland	0.03	0.56	8.31	12.27	1.07	4.40	18.33	68.79	
Shrubland	0.19	36.23	22.67	337.58	14.1	42.17	139.43	29.23	
Bare land	0.00	0.29	0.26	4.12	0.71	3.38	8.05	91.85	
Built-up	0.12	4.21	0.52	5.66	4.19	49.21	14.69	22.99	
Gains (km ²)	0.38	41.54	25.04	89.33	20.52	50.5	251.37		
Gains (%)	2.45	57.84	75.07	20.92	96.64	50.65			

Table 10

LCLU change matrix for 1988–2022 change period.

1988	LCLU classes	2022							
	Water bodies	Water bodies	Trees dominated	Cropland	Shrub land	Bare land	Built-up	Losses (km ²)	Losses %
Water bodies	14.59	0.76	1.09	4.69	0.97	0.08	7.60	34.24	
Trees dominated	0.44	31.53	2.70	105.78	2.10	5.64	116.66	78.72	
Cropland	0.04	1.99	4.30	23.22	0.93	2.86	29.04	87.10	
Shrubland	0.31	58.3	9.11	265.58	14.97	65.62	160.78	37.71	
Bare land	0.07	1.37	3.55	14.65	1.24	5.74	25.38	95.35	
Built-up	0.00	1.93	0.12	1.39	1.03	19.77	4.46	18.42	
Gains (km ²)	0.85	64.34	16.57	137.26	20.00	79.94	343.92		
% Gains	5.54	67.11	79.4	34.07	94.17	80.17			

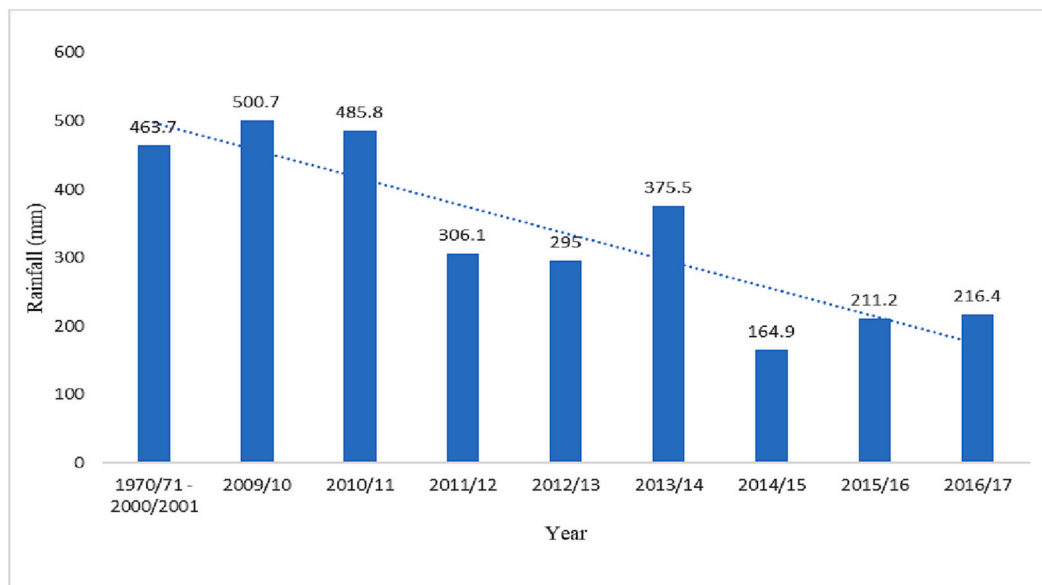


Fig. 6. National Average Rainfall (mm) (long vs short terms) [35].

Table 11
Annual rate of change in the area of LCLU Types.

LCLU type	1988–2002		2002–2022		1988–2022	
	Km ² per year	% per year	Km ² per year	% per year	Km ² per year	% per year
Water bodies	−0.19	−0.85	−0.21	−1.05	−0.2	−0.9
Trees dominated	−1.58	−1.22	−0.56	−0.52	−0.98	−0.76
Cropland	−1.34	−3.38	0.63	2.99	−0.18	−0.46
Shrubland	0.85	0.2	−1.8	−0.41	−0.71	−0.17
Bare land	−1.26	−4.74	0.63	7.08	−0.15	−0.56
Built up	3.53	14.56	1.29	1.75	2.21	9.12

shrubland class was observed (Fig. 5). Shrubland losses were primarily attributed to cropland and built-up classes. In addition, shrubland losses during this period could be attributed to a decrease in annual rainfall in the country over previous years (Fig. 6), as vegetation production in semi-arid regions is highly dependent on rainfall [34].

There was a general decrease in the area covered by the cropland class throughout the study period. While cropland area coverage decreased significantly between 1988 and 2002, there was a significant gain in its coverage between 2002 and 2022. The reduction in cropland coverage observed between 1988 and 2002 can be attributed to field abandonment due to the failure of agricultural support programs such as the Arable Land Development Program (ALDEP), and the Arable Rain-Fed Agricultural Program (ARAP) [36]. Abandonment of agricultural land has been reported to have increased globally and within Sub-Saharan Africa [37], despite the clear need for increased agricultural engagement and productivity. Cropland abandonment in Southern Africa, has been linked to the lack of draught power, variable rainfall, droughts and more modernized youths who are hesitant to live a marginal agrarian lifestyle [38].

This study showed that most of the croplands were located in rural areas (e.g., Oodi, Modipane, Tlokweng, Gabane and Mokolodi) and were rainfed. The rural population is typical of the entire Botswana in that it relies on rain-fed subsistence farming combined with livestock rearing [4]. The results indicate that agriculture remains the backbone of the rural economy, as evidenced by the observed gain in cropland between 2002 and 2022 (Fig. 5). This result concurred with the findings of Bessah et al. [39] who reported that the expansion of agricultural land is a global trend regardless, of the economic status and location of a country. The gains in cropland observed during the 2002–2022 period, could be attributed to the need for more food production towards meeting the demand of the growing population. In addition, it could also be attributed to the presence of agricultural subsidy schemes such as ISPAAD and other government support programs. One of the objectives of ISPAAD, was to provide farmers with a 100% subsidy for ploughing and row planting [40], thereby encouraging more farmers to clear more land for cultivation. The expansion in cropland contributed to the reduction in shrubland in the study area. Cropland expansion was also reported in the Ameleke watershed in Ethiopia in 2014 [41], as well as in other developing countries where the loss of natural vegetation for crop production was crucial [42].

Generally, water bodies shrank throughout the study period. A total of 6.77 km² (30.51%) of the water body class was lost between 1988 and 2022 (Fig. 5). The water body class was mainly losing to the shrubland class. The reduction in the area coverage of this LCLU type, is an indication of low rainfall and high evaporation. The water class expansively lost 4.12 km² of its area between 2002 and 2022, compared to 2.65 km² lost between 1988 and 2002. This could be attributed to usage and low rainfall in the country during that period.

3.4. Annual change rate

The annual change rates for the different LCLU types between 1988 and 2002, and 2002 and 2022 change periods are presented in Table 11. Overall, the fastest annual change rates in the different LCLU types, were

observed in the 1988–2002 change period, compared to the 2002–2022 change period. In addition, trees dominated LCLU class, was the most reduced category, as opposed to built-up, being the most increased category in the entire study period (1988–2022).

Between 1988 and 2002, the trees dominated class reduced annually at a rate of 1.58 km²/year (−1.22%/year), making it the most shrunk LCLU type in the period. Other LCLU categories whose annual change rates reduced during this period, include water bodies (−0.19 km²/year), cropland (−1.34 km²/year) and bare land (−1.26 km²/year). However, the built-up class increased annually at a rate of 3.53 km²/year (14.56% /year), making it the fastest-growing category in that period. This finding was in line with the findings of López et al. [43], who found that settlements in developing countries are growing five times faster than those in developed countries. Similarly, shrubland experienced an increased rate of change of 0.85 km² per year during this period.

With regards to the 2002–2022 change period, the area of water bodies, trees dominated and shrubland LCLU classes decreased by 0.21 km², 0.56 km², and 1.80 km² annually, respectively, while that of cropland, bare land, and built-up classes increased by 0.63 km², 0.63 km² and 1.29 km² per year, respectively. During this period, the shrubland class was the most shrunk category, whereas the built-up class was the highest increased category.

4. Conclusions

The Greater Gaborone area has undergone a considerable LCLU change over the past 34 years (1988–2022). The built-up LCLU type has increased significantly over this period, gaining a total of 75.12 km² from the other classes, with shrubland primarily contributing to this increase. The built-up annual increase was estimated as 2.21 km². On the other hand, trees dominated and shrubland LCLU types have decreased by 33.32 km² at a rate of 0.98 km² per year, and 24.16 km² at a rate of 0.71 km² per year, respectively. These changes are likely to negatively impact the environment and thus require some monitoring. This study recommends that land managers and policymakers should adopt appropriate land management strategies, such as conservation agricultural operations, discouraging overgrazing and limiting the conversion of natural vegetation to other land uses, for sustainable natural resources management. In addition, stakeholders should invest efforts to raise public awareness of the importance of environmental protection to prevent undesirable LCLU changes in the area.

Compliance with ethical standards

Not applicable.

Declaration of competing interest

The authors declare that they have no known competing financial interests or personal relationships that could have appeared to influence the work reported in this paper.

Acknowledgement

The authors wish to acknowledge the Mobile of African Scholars for Transformative Engineering Training (MASTET) scholarship for supporting this research.

References

- [1] B. Mathodi, P.K. Kenabatho, B.P. Parida, J.G. Maphanyane, Analysis of the future land use land cover changes in the Gaborone Dam catchment using CA-Markov Model: implications on water resources, *Remote Sens.* 13 (2021), <https://doi.org/10.3390/rs13132427>.
- [2] R.J. Permatasari, A. Damayanti, T.L. Indra, M. Dimiyati, Prediction of land cover changes in Penajam Paser Utara regency using cellular automata and markov model, in: *IOP Conf Ser Earth Environ Sci*, IOP Publishing Ltd, 2021, <https://doi.org/10.1088/1755-1315/623/1/012005>.
- [3] C. Liping, S. Yujun, S. Saeed, Monitoring and predicting land use and land cover changes using remote sensing and GIS techniques—a case study of a hilly area, Jiangle, China, *PLoS One* 13 (2018), <https://doi.org/10.1371/journal.pone.0200493>.
- [4] B. Mathodi, P.K. Kenabatho, B.P. Parida, J.G. Maphanyane, Evaluating land use and land cover change in the Gaborone dam catchment, Botswana, from 1984-2015 using GIS and remote sensing, *Sustainability (Switzerland)*. 11 (2019), <https://doi.org/10.3390/su11195174>.
- [5] F. Hossain, D.M. Moniruzzaman, Environmental change detection through remote sensing technique: a study of Rohingya refugee camp area (Ukhia and Teknaf sub-district), Cox's Bazar, Bangladesh, *Environ. Challeng.* 2 (2021), <https://doi.org/10.1016/j.envc.2021.100024>.
- [6] T.G. Adualem, G. Belay, A. Guadie, Land use change detection using remote sensing technology, *J Earth Sci Clim Change.* 9 (2018), <https://doi.org/10.4172/2157-7617.1000496>.
- [7] M. Pandian, G. Sakthivel, D. Amrutha, Land use and land cover change detection using remote sensing and GIS in parts of Coimbatore and Tiruppur districts, Tamil Nadu, India, *Int. J. Rem. Sens. Geosci. (IJRSG)*. 3 (2014). www.ijrsg.com.
- [8] E.F. Lambin, H.J. Geist, E. Lepers, Dynamics of land-use and land-cover change in tropical regions, *Annu. Rev. Environ. Resour.* 28 (2003) 205–241, <https://doi.org/10.1146/annurev.energy.28.050302.105459>.
- [9] H.J. Geist, E.F. Lambin, Proximate causes and underlying driving forces of tropical deforestation, *Bioscience.* 52 (2002) 143–150.
- [10] M.G. Munthali, Analysis of Land Use and Land Cover Change Dynamics and its Implications on Natural Resources in Dedza District, Malawi, 2020.
- [11] W. Chingombe, E. Pedzisai, R. Gondo, R. Mangizvo, Land use and land cover changes at Hova farm in Bindura District, Zimbabwe, *J Sustain Dev.* 14 (2021) 2021, <https://doi.org/10.5539/jsd.v14n4p42>.
- [12] Tobias Haller, Marc Galvin, Patrick Meroka, Jamil Alca, Alex Alvarez, Who gains from community conservation? Intended and unintended costs and benefits of participative approaches in Peru and Tanzania, *J. Environ. Dev.* 17 (2008) 118–144.
- [13] C. Vanderpost, S. Ringrose, Matheson Wilma, Aspects of ecological change in the Botswana Kalahari, *Botsw Notes Rec.* 30 (1998) 121–138.
- [14] R. Sebege, Historical Vegetation Changes in the Greater Gaborone Area. <https://www.researchgate.net/publication/237644346>, 2014.
- [15] Statistics Botswana, Population and Housing Census Preliminary Results V2, 2022, p. 2022.
- [16] B. Cavrić, M. Keiner, Managing Development of a Rapidly Growing African City: A Case of Gaborone, Botswana, 2006.
- [17] S.C. Neba, R. Tshoko, B. Kayombo, S.T. Moroke, Variation of soil organic carbon across different land covers and land uses in the greater Gaborone region of Botswana, *World J. Adv. Eng. Technol. Sci.* 07 (2022) 97–112, <https://doi.org/10.30574/wjaets.2022.7.2.0115>.
- [18] O. Dikinya, J. Athlopheng, T. Manyiwa, Variations on soil carbon dioxide flux with land-use type and selected soil properties in the hardveld of Botswana, *South African Journal of Plant and Soil.* 33 (2016) 309–316, <https://doi.org/10.1080/02571862.2016.1161091>.
- [19] R. Tshoko, Land cover land use (LCLU) classification methods in semi-arid Botswana, *J. Rem. Sens. GIS* 10 (2021) 497.
- [20] M.E. Madisa, Y. Assefa, O.D. Kelemoge, T. Mathowa, A.T. Segwagwe, Incidence and level of mistletoe infestation in tree species at Botswana University of Agriculture and Natural Resources' Sebele content farm campus, Botswana, *Int J Environ Agric Res.* 3 (2017) 53–58, <https://doi.org/10.25125/agriculture-journal-ijoe-ar-nov-2017-9>.
- [21] Statistics Botswana, Population and Housing Census 2022 Population of Cities, Towns and Villages, Gaborone. www.statsbots.org.bw, 2022.
- [22] D. Phiri, J. Morgenroth, C. Xu, Long-term land cover change in Zambia: an assessment of driving factors, *Sci. Total Environ.* 697 (2019), 134206, <https://doi.org/10.1016/J.SCITOTENV.2019.134206>.
- [23] P. Tendaupenyu, C.H.D. Magadza, A. Murwira, Changes in landuse/landcover patterns and human population growth in the Lake Chivero catchment, Zimbabwe, *Geocarto Int.* 32 (2017) 797–811, <https://doi.org/10.1080/10106049.2016.1178815>.
- [24] P. Mather, B. Tso, Classification Methods for Remotely Sensed Data, 2nd edition, CRC Press, Boca Raton, 2009, <https://doi.org/10.1201/9781420090741>.
- [25] D. Erasu, Remote sensing-based urban land use/land cover change detection and monitoring, *J. Rem. Sens. GIS.* 06 (2017), <https://doi.org/10.4172/2469-4134.1000196>.
- [26] M.G. Turner, Landscape Ecology in North America: Past, Present, and Future, 2005.
- [27] J.R. Jensen, D.C. Cowen, Remote sensing of urban/suburban infrastructure and socio-economic attributes, *Photogramm. Eng. Remote. Sens.* 5 (1999) 611–622.
- [28] B.M. Molla, C.O. Ikorukpo, C.O. Olatubara, The Spatio-temporal pattern of urban green spaces in southern Ethiopia, *Am. J. Geogr. Informat. Syst.* 2018 (2018) 1–14, <https://doi.org/10.5923/j.agis.20180701.01>.
- [29] R.D. Macleod, R.G. Congalton, A quantitative comparison of change-detection algorithms for monitoring eelgrass from remotely sensed data, *Photogramm. Eng. Remote. Sens.* 64 (1998) 207–216.
- [30] E.E. Hassen, M. Assen, Land use/cover dynamics and its drivers in Gelda catchment, Lake Tana watershed, Ethiopia, Hassen and Assen environ, *Syst. Res.* 6 (2017) 4, <https://doi.org/10.1186/s40068-017-0081-x>.
- [31] J.T. Fox, M.E. Vandewalle, K.A. Alexander, Land cover change in northern Botswana: the influence of climate, fire, and elephants on semi-arid savanna woodlands, *Land (Basel).* 6 (2017), <https://doi.org/10.3390/land6040073>.
- [32] F.O. Akinyemi, Climate change and variability in semi-arid Palapye, eastern Botswana: an assessment from smallholder farmers, *Perspective (2017)*, <https://doi.org/10.1175/WCAS-D-16-0040.s1>.
- [33] J. Byakatonda, B.P. Parida, D.B. Moalafhi, P.K. Kenabatho, Analysis of long-term drought severity characteristics and trends across semi-arid Botswana using two drought indices, *Atmos. Res.* 213 (2018) 492–508, <https://doi.org/10.1016/J.ATMOSRES.2018.07.002>.
- [34] H.N. le Houerou, R.L. Bingham, W. Skerbek, Relationship between the variability of primary production and the variability of annual precipitation in world arid lands, *J. Arid Environ.* 15 (1988) 1–18, [https://doi.org/10.1016/S0140-1963\(18\)31001-2](https://doi.org/10.1016/S0140-1963(18)31001-2).
- [35] Statistics Botswana, Botswana Environment Statistics Natural Disasters Digest 2017, Gaborone, www.statsbots.org.bw, 2018.
- [36] K.C. Seto, B. Güneralp, L.R. Hutyrta, Global forecasts of urban expansion to 2030 and direct impacts on biodiversity and carbon pools, *Proc. Natl. Acad. Sci. U. S. A.* 109 (2012) 16083–16088, <https://doi.org/10.1073/pnas.1211658109>.
- [37] R. Shackleton, C. Shackleton, S. Shackleton, J. Gambiza, Deagrarianisation and forest revegetation in a, biodiversity hotspot on the wild coast, South Africa, *PLoS One* 8 (2013) 76939, <https://doi.org/10.1371/journal.pone.0076939>.
- [38] D. Blair, C.M. Shackleton, P.J. Mograbi, Cropland Abandonment in South African Smallholder Communal Lands: Land Cover Change (1950–2010) and Farmer Perceptions of Contributing Factors 7, 2018, <https://doi.org/10.3390/land7040121>.
- [39] E. Bessah, A. Bala, S.K. Agodzo, A.A. Okhimamhe, E.A. Boakye, S.U. Ibrahim, The impact of crop farmers' decisions on future land use, land cover changes in Kintampo north municipality of Ghana, *Int J Clim Chang Strateg Manag.* 11 (2019) 72–87, <https://doi.org/10.1108/IJCCSM-05-2017-0114>.
- [40] GoB, Guidelines for Integrated Support Programme for Arable Agriculture Development (ISPAAD), Gaborone, 2013.
- [41] H. Temesgen, G. Worku, A. Bantider, Effects of land use/land cover change on some soil physical and chemical properties in Ameleke micro-watershed, Gedeo and Borena zones, South Ethiopia 4 (2014). www.iiste.org.
- [42] R.N. Lubowski, S. Bucholtz, R. Claassen, M.J. Roberts, J.C. Cooper, A. Gueorguieva, R. Johansson, Environmental Effects of Agricultural Land-Use Change United States Department of Agriculture the Role of Economics and Policy. www.ers.usda.gov, 2006.
- [43] E. López, G. Bocco, M. Mendoza, E. Duhau, Predicting Land-Cover and Land-Use Change in the Urban Fringe a Case in Morelia City, Mexico, 2001.